J. Biochem. 2011;150(4):411–421 doi:10.1093/jb/mvr071

JB THE JOURNAL OF BIOCHEMISTRY

Calpain-7 binds to CHMP1B at its second α-helical region and forms a ternary complex with IST1

Received March 11, 2011; accepted May 8, 2011; published online May 25, 2011

Yuki Maemoto, Yohei Osako, Emi Goto, Eri Nozawa, Hideki Shibata and Masatoshi Maki*

Department of Applied Molecular Biosciences, Graduate School of Bioagricultural Sciences, Nagoya University, Furo-cho, Chikusa-ku, Nagoya 464-8601, Japan

*Masatoshi Maki, Department of Applied Molecular Biosciences, Graduate School of Bioagricultural Sciences, Nagoya University, Nagoya 464-8601, Japan. Tel: +81-52-789-4088, Fax: +81-52-789-5542, email: mmaki@agr.nagoya-u.ac.jp

Some intracellular proteins involved in the endosomal sorting complex required for transport (ESCRT) system have microtubule interacting and transport (MIT) domains and bind to ESCRT-III protein family members named charged multivesicular body proteins (CHMPs) at their C-terminal regions containing MIT-interacting motifs (MIMs). While two types of MIMs (MIM1 and MIM2) have been reported, CHMP1B has MIM1 and IST1 has both MIM1 and MIM2. Previously, we demonstrated that CHMP1B and IST1 directly interacted with a tandem repeat of MIT domains of calpain-7 (CL7MIT) and that autolytic activity of calpain-7 was enhanced by IST1 *in vitro* but not by overexpression of IST1 in HEK293T cells. In this study, we detected enhancement of autolysis of mGFP-fused calpain-7 by coexpression with CHMP1B and observed further activation by additional coexpression of IST1 in HEK293T cells. We found that CL7MIT interacted with the second α-helical region of CHMP1B but not with the canonical C-terminal region containing MIM1 *in vitro*. Co-immunoprecipitation assays demonstrated that the interaction between CL7MIT and CHMP1B and between CL7MIT and IST1 became stronger when IST1 or CHMP1B was additionally coexpressed, suggesting formation of ternary complex of calpain-7, IST1 and CHMP1B. Moreover, subcellular fractionation analyses revealed increase of calpain-7 in membrane/organelle fractions by concomitant overexpression of these ESCRT-III family member proteins.

Keywords: calpain/CHMP/ESCRT/IST1/MIT domain.

Abbreviations: CBB, Coomassie Brilliant Blue R-250; CHMP, charged multivesicular body protein; CL7MIT, calpain-7 MIT domains; DTT, dithiothreitol; ESCRT, endosomal sorting complex required for transport; FBS, fetal bovine serum; EGF, epidermal growth factor; FL, full-length; GAPDH, glyceraldehyde-3-phosphate dehydrogenase; GST, glutathione-*S*-transferase; HEK, human embryonic kidney; IgG, immunoglobulin G; IP, immunoprecipitation; IST1, increased sodium tolerance 1; Lamp-1, lysosomal-associated membrane protein-1; LIP5MIT, LIP5 MIT domains; MIM, MIT interacting motif; MIT, microtubule interacting and transport; mAb, monoclonal antibody; NP-40, Nonidet P40; mGFP, monomeric green fluorescent protein; MVB, multivesicular body; pAb, polyclonal antibody; PBS, phosphate buffered saline; PEF, penta-EF-hand; PVDF, polyvinylidene difluoride; VPS, vacuolar protein sorting; WB, western blotting.

Endosomal sorting complex required for transport (ESCRT) machineries are composed of four complexes termed ESCRT-0, -I, -II and -III as well as an AAA-type ATPase VPS4 complex that dissociates ESCRT-III. Endocytosed plasma membrane receptors, such as the epidermal growth factor (EGF) receptor, are ubiquitinated and sequentially transferred from ESCRT-0, -I, -II to -III and transported to intraluminal vesicles of multivesicular bodies (MVBs) for lysosomal degradation (*1*, *2*). Other functions of ESCRT machineries in membrane deformation/fission events such as retrovirus budding and cytokinesis have also been reported (*3*). ESCRT-III protein family members named charged multivesicular body proteins (CHMPs) are thought to function as a membrane deformation apparatus. On the other hand, VPS4 complex interacts with ESCRT-III proteins via the microtubule interacting and transport (MIT) domain in VPS4 and dissociates ESCRT complexes from the endosomal membrane (*4*). X-ray crystal structure analyses have revealed that ESCRT-III proteins are composed of an N-terminal four-helix bundle core domain (α-helices1-4: α1–α4), an autoinhibitory helix (α5) and one or two regions of MIT-interacting motifs (MIMs) (*5*, *6*). Two types of MIMs with different structural features have been reported. While CHMP1A, -1B, -2A, -2B, and -3 have MIM1 that forms an amphipathic helix (*7*, *8*), CHMP4A, -4B, -4C and -6 have MIM2 that forms a Pro-rich strand (*9*). An ESCRT-III-related protein named IST1 has a CHMP-like domain on its N-terminal side and two MIMs in its C-terminal region, and both MIMs are thought to be involved in interaction with the VPS4 MIT domain (*10*, *11*).

Typical calpains, such as μ- and m-calpains, are intracellular Ca^{2+}-dependent cysteine proteases that proteolyze substrates at preferred cleavage sites (*12–14*). They are composed of catalytic large subunits and a common regulatory small subunit, which heterodimerize via a domain composed of five EF-hands

[penta-EF-hand (PEF)] present in both subunits (*15*, *16*). The large subunits contain a protease domain and a C2-like domain. An activation mechanism has been clarified by 3D structures of Ca^{2+}-free and Ca^{2+}-bound forms of typical calpains (*12–17*). Although the activation mechanism of calpains has not been completely elucidated, these typical calpains are expressed ubiquitously and have been suggested to play fundamental biological roles in the cell cycle and signal transduction (*14*, *18–20*). On the other hand, calpain-7, an atypical calpain that lacks the PEF domains, is the most conserved calpain among eukaryotes. Many studies on yeast (Cpl1/Rim13) and fungal (PalB) orthologues of calpain-7 have shown roles in the alkaline adaptation pathway (*21–23*), which utilizes a part of the ESCRT system (*24–26*).

We previously reported that a tandem repeat of human calpain-7 MIT domains (CL7MIT) interacted with IST1 at its MIMs (IST1MIMs) and that glutathione-*S*-transferase (GST)-fused IST1MIMs enhanced autolytic activity of strep-tagged mGFP-calpain-7 (mGFP-calpain-7-Strep) *in vitro*. However, overexpression of IST1 in HEK293T cells did not enhance autolysis of mGFP-calpain-7 (*27*). We assumed that IST1 is not a limited factor in cells but that there is an unknown cooperating factor to promote calpain-7 activities. While we have reported physical interactions between CHMP1B and calpain-7 (*28*), other groups have found that CHMP1B interacts with IST1 (*10*, *11*, *29*, *30*). These findings led us to investigate whether CHMP1B is an activating cofactor of calpain-7 in cells. In this study, we found that overexpression of CHMP1B enhanced mGFP-clapain-7 autolysis in the expression plasmid-transfected HEK293T cells and that additional coexpression of IST1 further enhanced its autolytic activity. We also found that C-terminal deletion mutants of CHMP1B enhanced autolytic activity of calpain-7 in cells and that the MIT domain of calpain-7 bound to the predicted α2 region in CHMP1B but not to the C-terminal α6 containing MIM, which is known as the binding site for VPS4 MIT.

Materials and Methods

Antibodies and reagents

The following mouse monoclonal antibodies (mAbs) were used: anti-FLAG mAb (clone M2, Sigma, St Louis, MO, USA) and anti-GFP (green fluorescent protein) mAb (clone B-2, Santa Cruz Biotechnology, Santa Cruz, CA, USA), anti-CD107a/Lamp1 mAb (Pharmingen, Palo Alto, CA, USA) and anti-GAPDH mAb (Chemicon, Bilerica, MA, USA).

Polyclonal antibody (pAb) against recombinant human IST1 was raised in rabbits using 6xHis-tagged IST1 (His-IST1) as an antigen and affinity purified using GST-IST1 that had been immobilized to Sepharose beads. Rabbit pAb against recombinant human CHMP1B was raised in rabbits using GST-CHMP1BΔNT (*28*) and affinity purified using Trx-CHMP1BΔNT-immobilized Sepharose beads. Anti-GFP anti-serum (catalogue no. A6455) was obtained from Invitrogen/Molecular Probes (Carlsbad, CA, USA). Rabbit pAb against the recombinant GST-fused MIT domain of human calpain-7 was obtained as described previously (*28*).

Plasmid constructions

Constructions of the following plasmids were described previously: monomeric enhanced GFP (mGFP)-fused calpain-7 (mGFP-calpain-7), mGFP-CL7MIT, mGFP-CHMP1B, FLAG-CHMP1B, FLAG-CHMP3 FLAG-IST1 and bacterial expression plasmids for GST-MIT-pHis and GST-IST1 (*27*, *28*). To construct a GST-fused protein expression vector, a DNA fragment of GST including its multi-cloning site was amplified by PCR using pGEX4T-3 (GE Healthcare, Buckinghamshire, England) as a template and a pair of primers (forward, GGAGCCATGGCCCTATA CTAGGTTATT; reverse, TTCTCCTTGGTCAGTCAGTCACGA TGCGG; *Eco*T14I sites underlined). The *Eco*T14I-digested fragment was inserted into the *Eco*T14I site of pET24d (Novagen, Darmstadt, Germany) and the resultant vector was named pET24-GST. Bacterial expression plasmids for GST-CHMP1A and GST-CHMP1B were constructed as follows: the DNA fragments encoding CHMP1A and CHMP1B were amplified by PCR using cDNA encoding CHMP1A and CHMP1B as templates and a pair of primers (1A: forward, GGTTCCGCGTGGATCCGACGATACCCT GTTCCAG; reverse, GATGCGGCCGCTCGAGGGTCGAGCT AGTTCCTC; 1B: forward, GGTTCCGCGTGGATCCTCTAAC ATGGAGAAACACCTGT; reverse, GATGCGGCCGCTCGAG TCG; restriction sites underlined). The PCR product was inserted into the *Bam*HI- and *Xho*I-digested pET24-GST vector using an In-Fusion® Advantage PCR Cloning Kit (Clontech, Palo Alto, CA, USA). Bacterial expression plasmids for GST-CHMP1B mutants except for GST-CHMP1BΔNt were obtained by PCR-based site-directed mutagenesis using specific primers (Supplementary Table 1) and pET24-GST-CHMP1B as a template. Deletion mutants of CHMP1B in this study are schematically shown in Fig. 1. To construct mammalian expression vectors of pFLAG-CHMP1B mutants and pmGFP-CHMP1Bα1, the same primers as those described above were used for mutagenesis. The mutations were confirmed by nucleotide sequencing. To construct pGST-CHMP1BΔNt, a cDNA fragment encoding 68–199 amino acids was amplified by PCR using primers as described previously (*28*) and the fragment was inserted into the *Eco*RI/*Sal*I site of pGEX4T-1 vector (GE Healthcare, Buckinghamshire, England). For a bacterial expression plasmid for GST-LIP5MIT, a cDNA fragment corresponding to a part of LIP5 protein (1–168 amino acids) was amplified by PCR using a cDNA

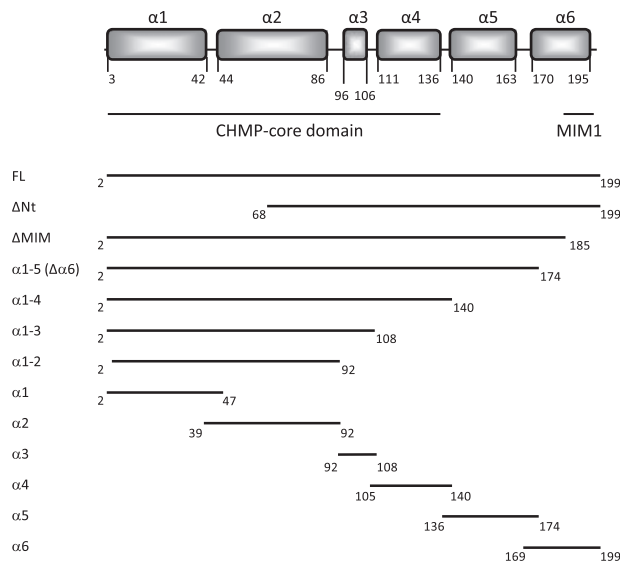

Fig. 1 Schematic representations of CHMP1B. CHMP1B has six predicted α-helices (α1–6). The N-terminal domain (α1–5) is conserved among CHMP proteins and C-terminal α6 contains MIM1. The upper constructs are C-terminal deletion mutants except for ΔNt, and lower constructs are segments composed of each α-helix and its surrounding sequences. The numbers below the bars indicate positions in amino acid residues. FL, Full-length. Secondary structure of the core domain of CHMP1B (α1–4) was predicted by alignment with CHMP3 whose 3D structure was determined (*5*, PDB ID: 2gd5). The C-terminal two α-helices of CHMP1B were taken from the 3D structure of the complex between the C-terminal fragment of CHMP1B and the MIT domain of spastin (*32*, PDB ID: 3eab).

clone (accession no: BC022536) obtained from Open Biosystems Institute (Huntsville, AL, USA) and a pair of primers (forward, TCTGAATTCATGGCCGCGCTTGCACC; reverse, TCTGAATTCATTGAGGAGTCTCCCCATTC; stop codon italicized and *Eco*RI sites underlined). The amplified cDNA fragment was first inserted into the Zero Blunt TOPO PCR Cloning vector (Invitrogen), and then the *Eco*RI-digested fragment was inserted into the *Eco*RI site of pmGFP-C2 (*31*). From this intermediate construct, a DNA fragment of LIP5MIT was isolated by *Bgl*II/*Bam*HI digestion, and inserted into the *Bgl*II site of pGST-PreScission-*Bgl*II-PreScission-His (*27*).

A pair of oligonucleotides encoding the 4xGGS sequence (forward, GTACAAAGGAGGAAGCGGAGGCTCTGGCGGTTCC GGAGGTTCACA; reverse, GATCTGTGAACCTCCGGAACCG CCAGAGCCTCCGCTTCCTCCTTT) was inserted into the *Bsp*EI/*Bgl*II site of pmGFP-C2 and the resultant plasmid was named pmGFP-GGS. The DNA sequence of the multiple-cloning site followed by universal translation terminators encodes 22 amino acids after the GGS linker. DNA fragments for CHMP1B α-helices obtained by PCR using specific primers except for CHMP1Bα3 and a pair of oligonucleotides encoding CHMP1Bα3 were inserted into the *Xho*I site of pmGFP-GGS. Primers used for CHMP1B α-helices are shown in Supplementary Table 2.

Cell culture

HEK293T cells were cultured in Dulbecco's modified Eagle's medium (DMEM) supplemented with 5% fetal bovine serum (FBS), 100 U/ml penicillin and 100 μg/ml streptomycin at 37°C under humidified air containing 5% CO_2.

Expression and purification of recombinant proteins and GST pull-down assay

Escherichia coli BL21 and BL21 (DE3) cells were transformed with each expression plasmid for GST fusion protein (pGST, pGST-IST1, pGST-pHis, pGST-CL7MIT-pHis, pGST-CL7MIT, pGST-LIP5MIT, pGST-CHMP1A, pGST-CHMP1B and pGST-CHMP1B mutants). Expression of GST-IST1, -CHMP1A, -CHMP1B and -CHMP1B mutants was induced with 0.5 mM isopropyl-1-thio-β-D-galactopyranoside (IPTG) for 3 h at 30°C, and the GST fusion proteins were purified with glutathione-Sepharose 4B (GE Healthcare) beads according to the manufacturer's instructions. GST-CL7MIT and -LIP5MIT were expressed and purified essentially in the same way as described above except for its induction time (overnight). Purified proteins were dialysed against phosphate buffered saline (PBS) (137 mM NaCl, 2.7 mM KCl, 8 mM Na_2HPO_4 and 1.5 mM KH_2PO_4, pH 7.3) and stored at 4°C until use. Expression and purification of GST-pHis and GST-MIT-pHis and recombinant CL7MIT were described previously (*27*).

GST pull-down assay from mammalian cell lysates

At 24 h after transfection of approximately 6×10^6 HEK293T cells with expression vectors by the conventional calcium phosphate precipitation method, cells were washed with PBS, and harvested cells were lysed in 1 ml of buffer A (10 mM HEPES–NaOH, pH 7.4, 142.5 mM KCl, 0.2% NP-40) supplemented with protease inhibitors (0.4 mM phenylmethylsulphonyl fluoride, 0.2 mM pefabloc, 6 μg/ml leupeptin, 2 μM E-64 and 2 μM pepstatin) and 5 mM β-mercaptoethanol. Three hundred microlitres of supernatants (cleared lysates) obtained by centrifugation at 15,000*g* were incubated with glutathione-Sepharose beads immobilizing 10 μg of each GST fused protein for 2 h at 4°C with gentle mixing. After Sepharose beads had been recovered by low-speed centrifugation (700*g*) for 1 min and washed three times with buffer A, proteins bound to the beads (pull-down products) were subjected to SDS–PAGE followed by western blot (WB). Proteins transferred to polyvinylidene difluoride (PVDF) membranes (Immonobilon-P, Millipore, Bedford, MA, USA) were probed with appropriate antibodies. Chemiluminescent signals of western blotting (WB) were detected by a LAS-3000mini lumino-image analyser (Fujifilm, Tokyo, Japan) using Super Signal West Pico Chemiluminescent Substrate (Thermo Fisher Scientific Inc., IL, USA). Bands of GST fusion proteins were detected by staining the membranes with Coomassie Brilliant Blue R-250 (CBB).

In vitro binding assay using recombinant proteins

Ten micrograms each of GST (negative control), GST-IST1 (positive control), GST-CHMP1A, GST-CHMP1B and GST-CHMP1B mutants were immobilized on glutathione-Sepharose beads and mixed with 10 μg of recombinant CL7MIT proteins diluted in 400 μl of buffer B (50 mM Tris–HCl, pH 8.0, 350 mM NaCl, 0.2% NP-40 and 1 mM DTT) for 1 h at 4°C. After Sepharose beads had been pelleted by brief centrifugation and washed three times with buffer B (pull-down products), protein mixtures were separated on a 15% gel by SDS–PAGE. Initial protein mixtures (input) were detected by staining with CBB and pull-down products were subjected to WB with anti-calpain-7 pAb.

Co-immunoprecipitation assay

One day after HEK293T cells had been seeded, cells were transfected with mGFP-fused and FLAG-tagged protein expression plasmid DNAs. After 24 h, cells were harvested with PBS and lysed in buffer A containing protease inhibitors as described above. The lysates were incubated sequentially with anti-GFP anti-serum for 2 h and with Protein G-Sepharose 4 Fast Flow (GE Healthcare) at 4°C for 2 h, and then the beads were washed three times with buffer A and bound proteins were subjected to WB using appropriate antibodies as described above.

Subcellular fractionation

After transfection with either a FLAG-tag vector (Ctrl), pFLAG-CHMP1B, pFLAG-IST1 or both pFLAG-CHMP1B and pFLAG-IST1, HEK293T cells were harvested, suspended in buffer C (10 mM HEPES–KOH, pH 7.6, 10 mM KCl, 1.5 mM $MgCl_2$, 0.1 mM pefabloc, 25 μg/ml leupeptin, 1 μM E-64, 1 μM pepstatin), and homogenized by passing 20 times through a 26-gauge needle. The supernatant (S) and pellet (P) fractions were obtained by centrifugation at 10,000*g* for 15 min. Alternatively, plasmid-transfected HEK293T cells were lysed with buffer D (10 mM HEPES–NaOH, pH 7.4, 142.5 mM KCl, 1% Triton X-100) and centrifuged at 15,000*g* for 15 min. Total cell lysates (T), S and P fractions were subjected to SDS–PAGE and WB as described above. Signals for immunoreactive bands were quantified using Multi Gauge ver3.X (Fujifilm).

Results

Effects of CHMP1B and its mutant on autolytic activity of mGFP-calpain-7 in the expression plasmid transfected cells

In our previous studies, expression of mGFP-calpain-7 in HEK293T cells generated ~30, 45 and 60-kDa autolytic fragments (designated 30K, 45K and 60K, respectively), and those bands were not detected in the case of its inactive mutants (mGFP-calpain-7^{C290S}) (*27*). We also reported that binding ability of IST1 to calpain-7 is the strongest among ESCRT-III- and ESCRT-III-related proteins and that IST1 enhanced autolytic activity of mGFP-calpain-7-Strep *in vitro*, though overexpression of IST1 did not enhance autolytic activity in cells (*27*). Secondly to IST1, CHMP1B bound to calpain-7 more efficiently among ESCRT-III protein family members in previous interaction analyses (*27*, *28*). Calpain-7–CHMP1A interaction was also detected in one of those studies, but it was weaker than calpain-7–CHMP1B interaction under the conditions used (*28*). Studies on spastin MIT domain showed that spastin MIT interacted with CHMP1B but not with CHMP1A (*32*). Therefore, we focused on CHMP1B in this study. To investigate whether CHMP1B affects autolytic activity of mGFP-calpain-7 in cells, we first coexpressed FLAG-CHMP1B with mGFP-calpain-7 in HEK293T cells and analysed the total cell lysates by western

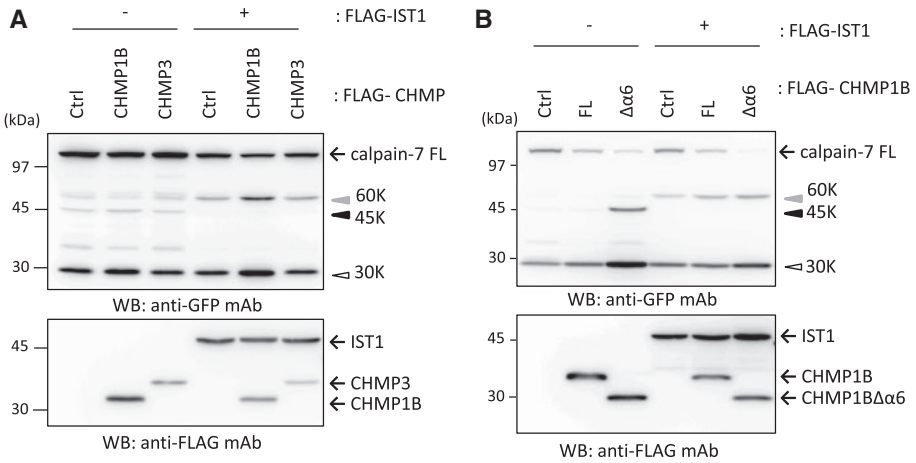

Fig. 2 Enhancement of autolytic activity of mGFP-calpain-7 by CHMP1B in cells. pmGFP-calpain-7 was cotransfected with pFLAG-tagged CHMP or a blank vector (Ctrl) indicated above the panels into HEK 293T cells. (A) CHMP1B and CHMP3, (B) CHMP1B wild type and mutant. Total cell lysates were subjected to SDS–PAGE and WB with anti-GFP mAb (upper panels) and anti-FLAG mAb (lower panels), respectively. Bands of full-length (FL), 60 kDa (60K), 45 kDa (45K) and 30 kDa (30K) are indicated by an arrow and grey, closed and open triangles, respectively. FL, Full-length.

blotting (WB) using anti-GFP mAb. Coexpression with CHMP1B generated slightly more 30K than did coexpression with CHMP3 (negative control) (Fig. 2A, upper panel, open arrowhead). We investigated effects of coexpression of CHMP1B with IST1 on the autolysis of mGFP-calpain-7 since CHMP1B is known to bind IST1 (*10*, *11*). The production of 60K and 30K was significantly enhanced with decrease in full-length mGFP-calpain-7, but other combinations of coexpression were not effective (Fig. 2A, upper panel, grey and open arrowheads).

The MIT domain of VPS4 is known to interact with CHMP proteins by recognizing MIT-interacting motifs (MIMs) present in the C-terminal region of each CHMP protein except for CHMP5 (*33*). We previously reported that CL7MIT bound IST1 at its C-terminal MIMs (MIM1 and MIM2) and that an IST1 mutant-lacking MIMs (IST1ΔMIM1, *2*) still possessed a weak binding ability to CL7MIT and suppressed autolysis of calpain-7 (*27*). To determine whether the enhancing activity of CHMP1B for mGFP-calpain-7 autolysis correlates with calpain-7–CHMP1B interaction, CHMP1BΔα6 lacking MIM1 (Fig. 1) was coexpressed with mGFP-calpain-7. Although the mutant was not expected to interact with CL7MIT, the coexpression produced a larger amount of autolytic bands of mGFP-calpain-7 than did coexpression with wild-type CHMP1B (Fig. 2B). Additional coexpression with IST1 did not show an apparent synergistic effect on enhancement of autolysis except for further decrease in the amount of full-length mGFP-calpain-7 in the case of CHMP1BΔα6. Coexpression with IST1 also caused changes in autolysis patterns: disappearance of 45K and appearance of 60K. Appearance of 60K may relate with the nature of autolysis (see discussion below).

GST-MIT pull-down assay of CHMP1B

Since CHMP1BΔα6 enhanced autolytic activity of calpain-7, we speculated that CL7MIT bound to CHMP1B in a region other than the C-terminal MIM. To investigate whether CHMP1BΔMIM interacts with CL7MIT, we performed pull-down assays using GST-fused CL7MIT (Fig. 3). Since LIP5, a regulatory protein of VPS4, has a tandem repeat of MIT domains (LIP5MIT), GST-LIP5MIT was used for comparison. Purified GST-MITs were immobilized on glutathione-Sepharose beads and incubated with lysates of HEK293T cells expressing CHMP1B or CHMP1BΔMIM. After incubation, cleared lysates (Input, left panel) and proteins bound to the beads (pull-down products) were separated by SDS–PAGE and subjected to WB using anti-FLAG mAb (pull-down, upper panels). Pull-down products were also visualized with CBB staining (CBB, lower panel). LIP5MIT pulled down CHMP1B (FL) but did not pull down CHMP1BΔMIM. In contrast, CL7MIT pulled down both CHMP1B and CHMP1BΔMIM, and the amount of CHMP1BΔMIM pulled down was larger than that of CHMP1B. As for GST (negative control, Ctrl), no immunoreactive bands were detected under the conditions used. Since spastin MIT needs an additional sequence adjacent to the N-terminal side of MIM1 in α6 of CHMP1B for binding (*32*), the entire sequence of α6 was assumed to be involved in interaction with CL7MIT. However, the binding ability of calpain-7 was not significantly different between CHMP1BΔMIM (1–185) and CHMP1BΔα6 (1–174) (Supplementary Fig. 1).

We speculated that calpain-7 bound to CHMP1B by recognizing a short sequence other than C-terminal MIM. To identify a binding site for CL7MIT in CHMP1B, we constructed monomeric GFP (mGFP)-fused CHMP1B mutants including each predicted α-helix shown in Fig. 1 with a flexible 4xGGS linker. GST-MIT pull-down assays were performed using lysate from cells expressing mGFP-CHMP1B α-helix mutants, which were expressed at similar levels (Fig. 4, input, left panel). As shown in the right panels of Fig. 4 for pull-down product analysis, GST-LIP5MIT interacted with mGFP-CHMP1Bα6 containing MIM (middle panel, doublet bands probably due to

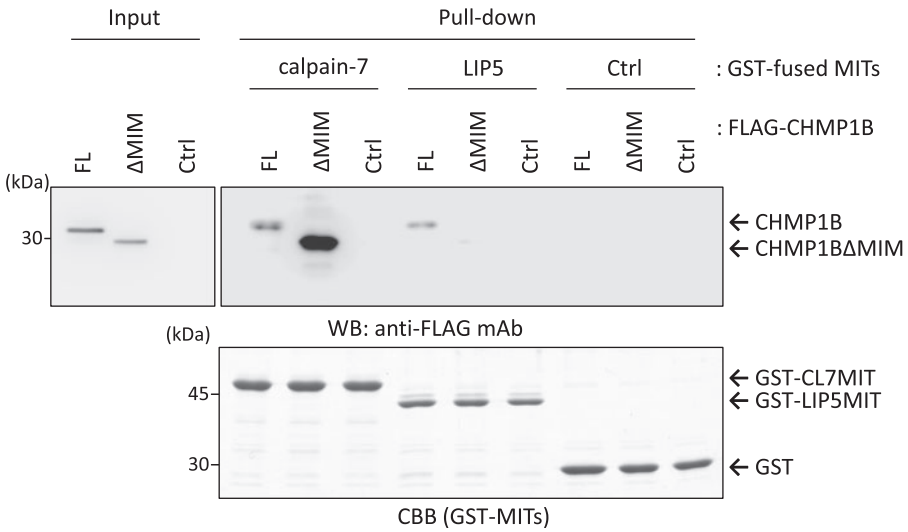

Fig. 3 GST-MIT pull-down assays of FLAG-CHMP1B and FLAG-CHMP1BΔMIM. HEK293T cells were transfected with pFLAG-CHMP1B (FL), pFLAG-CHMP1BΔMIM (ΔMIM) and pFLAG vector (Ctrl) as a negative control. At 24 h after transfection, cells were lysed, and the cleared lysates were incubated with recombinant GST-fused CL7MIT, LIP5MIT, or unfused GST (negative control, Ctrl) that had been immobilized on glutathione-Sepharose beads. The beads were then pelleted by low-speed centrifugation and washed with lysis buffer. The cleared lysates (input) and proteins in the pellets (pull-down product, pull-down) were subjected to SDS–PAGE and WB with anti-FLAG mAb. Immunoreactive bands were detected by the chemiluminescence method (upper panels). Input, 6% (analysis of 1.1% of total protein corresponding to 18% of pull-down products). The gel of pull-down products was also stained with CBB (lower panel).

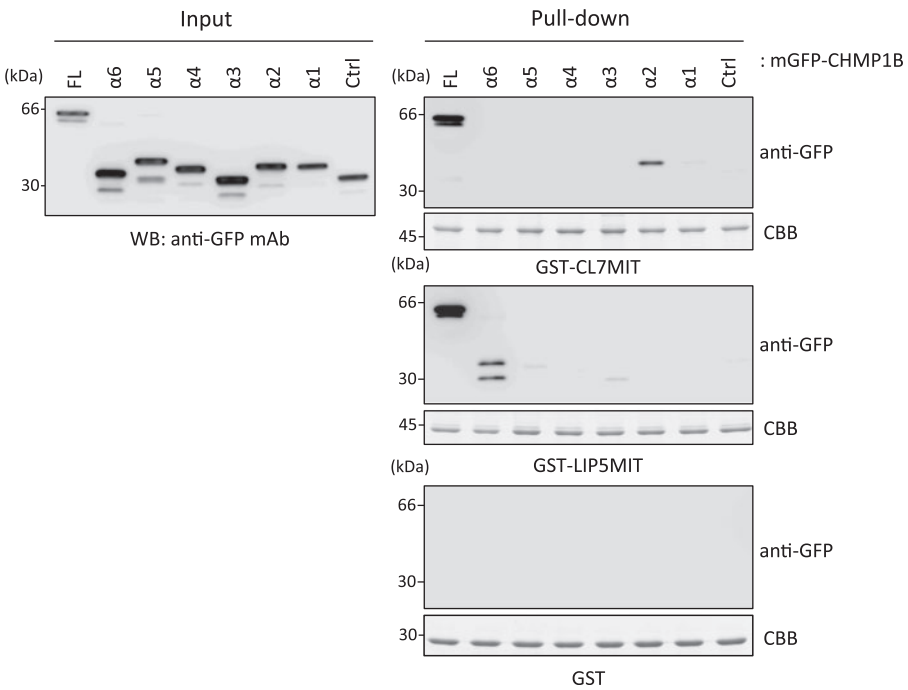

Fig. 4 GST-MIT pull-down assays of mGFP-CHMP1B α-helices. HEK293T cells were transfected with pmGFP-CHMP1B (FL), pmGFP-CHMP1B α-helices (Fig. 1) and pmGFP-GGS as a negative control (Ctrl). At 24 h after transfection, cells were lysed, and the cleared lysates were incubated with recombinant GST-fused tandem repeat of CL7MIT (right top panels), LIP5MIT (right middle panels) and unfused GST (right bottom panels) that had been immobilized on glutathione-Sepharose beads. The beads were then pelleted by low-speed centrifugation and washed with lysis buffer. The cleared lysates (Input, left panel) and proteins in the pellets (pull-down product, pull-down, right panels) were subjected to SDS–PAGE and WB with anti-GFP mAb. The gels of pull-down products were also stained with CBB (lower panels). Immunoreactive bands were detected by the chemiluminescence method (upper panels). Input, 7.5% (analysis of 1.9% of total protein corresponding to 25% of pull-down products).

N-terminal truncation of mGFP). On the other hand, GST-CL7MIT interacted with mGFP-CHMP1Bα2 containing 39–92 amino acids of CHMP1B but not with mGFP-CHMP1Bα6 (top panel).

Direct interaction between recombinant CL7MIT and GST-CHMP1B proteins

Since the results of all GST pull-down assays shown in Figs 3 and 4 were obtained by using cleared lysates of

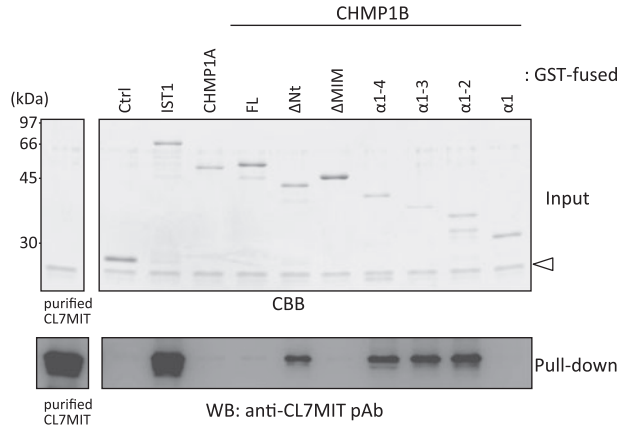

Fig. 5 *In vitro* binding assays using recombinant CL7MIT and GST-CHMP1B mutants. Purified recombinant CL7MIT (1–165 amino acids), CL7MIT, was incubated with GST (negative control, Ctrl), GST-IST1 (positive control), GST-CHMP1A, GST-CHMP1B (FL) and its mutants (Fig. 1) that had been immobilized on glutathione-Sepharose beads and subjected to GST pull-down assays. Purified CL7MIT (left panels), initial protein mixtures (input, right upper panel) and pull-down products (pull-down, right lower panel) were resolved on 15% gels by SDS–PAGE and subjected to CBB staining (upper panels) or WB using anti-CL7MIT pAb (lower panels). Open triangle indicates bands of recombinant CL7MIT. Input, 3.8% (analysis of 0.95% of total protein corresponding to 25% of pull-down products).

HEK293T cells, there remained the possibility that unknown factors might mediate CL7MIT–CHMP1B interaction. To exclude this possibility, we performed *in vitro* GST pull-down assays using purified recombinant CL7MIT and GST-fused CHMP1B mutants (Fig. 5). Immunoreactive bands for CL7MIT were barely detected or not detected in the pull-down products by GST-CHMP1A, GST-CHMP1B (FL), GST-CHMP1BΔMIM and GST-CHMP1Bα1 in comparison with GST (negative control, Ctrl). However, bands were detected in pull-down products of GST-CHMP1BΔNt, GST-CHMP1Bα1-4, GST-CHMP1Bα1-3 and GST-CHMP1Bα1-2, though intensities were weaker than GST-IST1 (positive control). Considering amino acid sequences of CHMP1BΔNt (68–199 amino acids) and CHMP1Bα1-2 (2–92 amino acids), the binding site for calpain-7 in CHMP1B should exist between 68 and 92 amino acids To demonstrate this possibility, we expressed GST-fused CHMP1Bα2 in bacterial cells, but it was so susceptible to degradation in bacterial cells that we could not use it for *in vitro* binding assays.

Enhancement of interaction between CL7MIT and CHMP1B by IST1

In the GST pull-down assays using GST-CL7MIT and cleared cell lysates, FLAG-CHMP1BΔMIM was efficiently pulled down, whereas no interaction was observed between CL7MIT and CHMP1BΔMIM mutant in the pull-down assays using both recombinant proteins *in vitro*. These discrepant results may reflect conformational differences of CHMP1B between *in vitro* and in cells. Since CHMP proteins form open and closed conformations by the core CHMP domain composed of α1–α4 *(6*, *34*, *35)*, the calpain-7-binding site at α2 may be sequestered under the *in vitro* assay conditions but exposed in cells. As cellular factors may induce conformational change of CHMP1B to interact with calpain-7, the most likely candidate seems to be IST1 because coexpression with CHMP1B enhances autolysis of mGFP-calpain-7 and IST1 also interacts with calpain-7 (Fig. 2, *27*). To investigate this possibility, we performed a co-immunoprecipitation assay of mGFP-CL7MIT by coexpressing either FLAG-CHMP1B or FLAG-IST1 alone or both FLAG-CHMP1B and FLAG-IST1. As shown in the upper right panels of Fig. 6, immunoreactive bands for both CHMP1B and IST1 are faint but above the background signals by mGFP (negative control) in the case of their single expression. However, bands for CHMP1B and IST1 were significantly enhanced by their coexpression in spite of similar expression levels (input, upper left panels).

Subcellular localization of calpain-7, CHMP1B and IST1

To investigate biological significance of the interaction of calpain-7 with the ESCRT-III-related proteins, we first performed a rough subcellular fractionation in the absence of non-ionic detergent by single high centrifugation at 10,000*g* of the lysates of HEK293T cells that had been transfected with expression plasmids for either FLAG-tagged IST1 or CHMP1B or both. Obtained fractions of 10,000*g* pellets (P) and 10,000*g* supernatants (S) were analysed by SDS–PAGE followed by WB using specific antibodies. A representative result of three independent experiments is shown in Fig. 7A. Marker proteins of late endosome/lysosome (Lamp-1) and cytosol (GAPDH) showed expected distribution patterns, which were not affected by overexpression of FLAG-CHMP1B and FLAG-IST1. On the other hand, the relative amount of endogenous calpain-7 in P fraction was increased in cells that overexpressed these proteins when compared with control cells that were transfected with empty vector (Ctrl), and this increase ($40.5 \pm 5.1\%$ vs $26.2 \pm 3.3\%$) was statistically significant ($P < 0.01$, Panel C). However, overexpression of exogenous CHMP1B or IST1 alone did not increase the amount of calpain-7 in P fraction. Increases in relative amounts of FLAG-CHMP1B and FLAG-IST1 as well as endogenous IST1 in P fractions were observed in cells by overexpressing both proteins (A, second and fourth panels from the top). Endogenous CHMP1B could not be detected by WB (A, third panel from the top). Lysis of cells in the presence of 1% Triton X-100 solubilized most calpain-7 and Lamp-1 (Panel B), and 3–6% of calpain-7 remained in P fractions (Panel C).

Next, we performed immunofluorescence microscopic analyses to investigate effects of overexpression of IST1 and CHMP1B on subcellular distributions of calpain-7. Fluorescence signals attributable to overexpressed Strep-IST1 (probed with anti-IST1 pAb) and GFP-CHMP1B (detected by GFP fluorescence) showed punctate distribution around nucleus and merged with the signals of FLAG-calpain-7^{C290S} (Supplementary Fig. 2, Panels E–L). In control experiments, fluorescence signals of FLAG-calpain-7^{C290S}

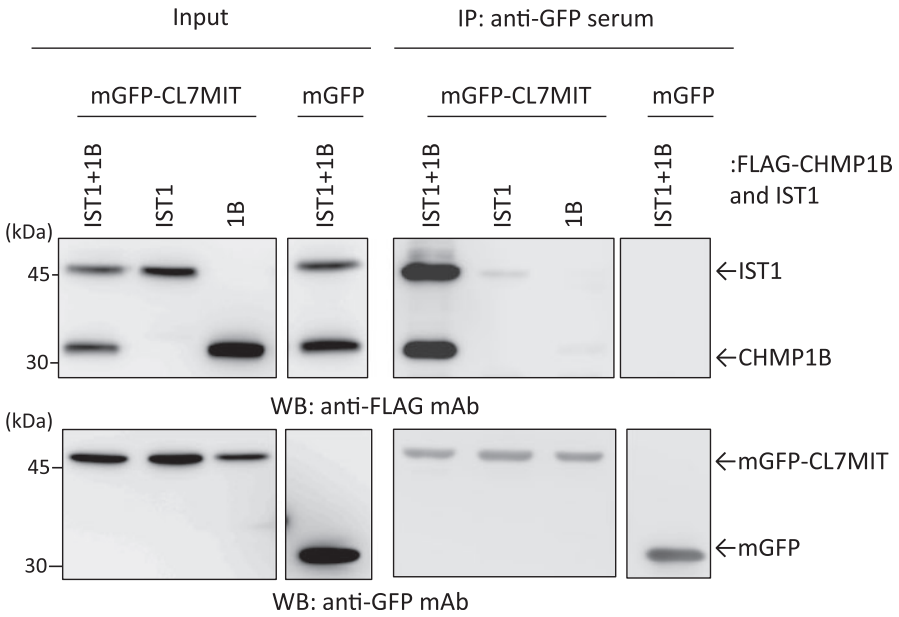

Fig. 6 Co-immunoprecipitation of FLAG-IST1 and -CHMP1B with mGFP-CL7MIT. HEK293T cells were transfected with pmGFP-CL7MIT, pFLAG-IST1 and pFLAG-CHMP1B as indicated above the panels. At 24 h after transfection, cleared cell lysates (input, left panels) were subjected to immunoprecipitation (IP, right panels) with anti-GFP serum followed by WB with anti-FLAG mAb (upper panels) and anti-GFP mAb (lower panels), respectively. Input, 3% (analysis of 0.54% of total protein corresponding to 18% of IP products).

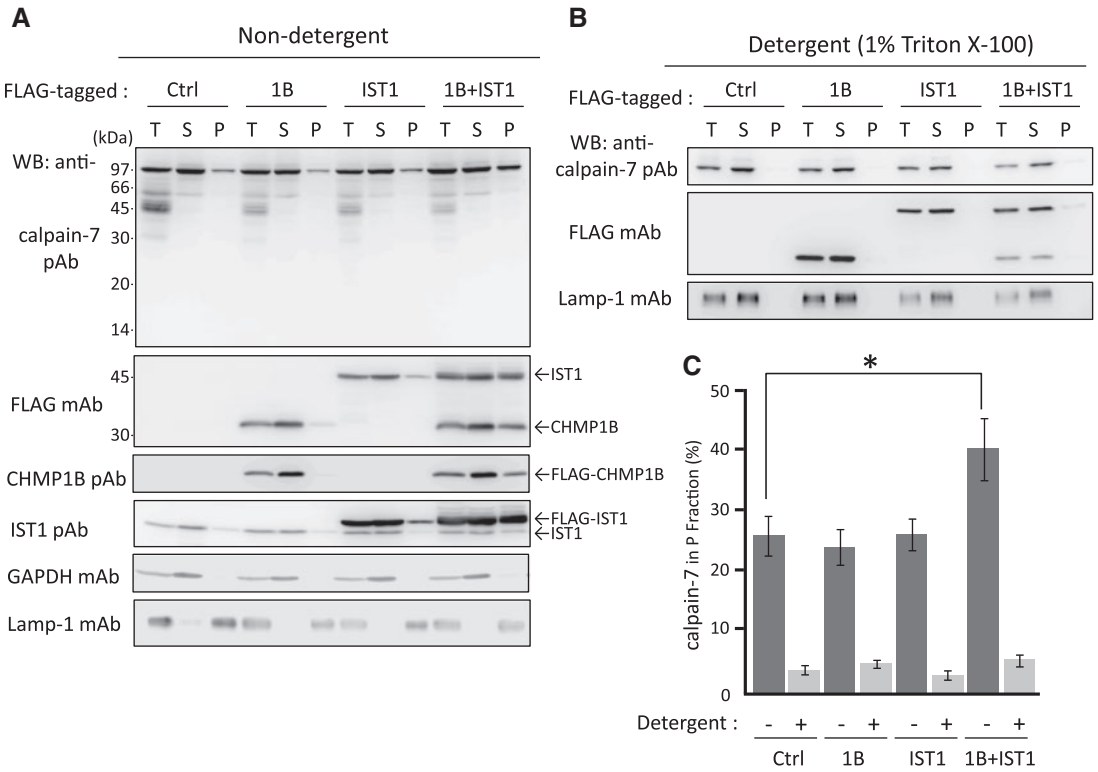

Fig. 7 Effects of overexpression of CHMP1B and IST1 on subcellular localization of endogenous calpain-7. (A) After HEK293T cells were transfected with expression plasmids for FLAG-tagged proteins (CHMP1B and IST1), or a blank vector (Ctrl) shown above the panels, cells were homogenized and fractionated by centrifugation at 10,000*g* as described in Materials and Methods section. Fractions of P (cell debris and a crude nuclear, mitochondrial and organelle-enriched pellet) and S (10,000*g* supernatant) as well as total cell lysate (T) were subjected to WB analyses using antibodies indicated. (B) Transfected cells were lysed with buffer containing 1% Triton X-100 and fractionated into supernatants (S) and pellet (P) by centrifugation at 15,000*g*. Fractions were similarly analysed by WB. (C) The intensities of signals of endogenous calpain-7 in S and P fractions were estimated by densitometry and relative amounts of calpain-7 in P fraction were calculated using following equation: $100 \times P/(S+P)$. The difference between overexpression of CHMP1B-IST1 and vector is highly significant. $^{*}P < 0.01$. Values are expressed as means of three independent experiments ± SEM.

(Panel A) also showed puncta and the signals partly merged with those for endogenous IST1 (Panel C), but the degree of colocalization was much less than the case of coexpression of the three individual proteins.

Discussion

Human calpain-7 has a tandem repeat of microtubule-interacting and transport (MIT) domains (CL7MIT), and we previously reported that CL7MIT interacts with IST1, CHMP1B, CHMP1A and to lesser extent to CHMP4b, CHMP4c, CHMP2A and CHMP7 but does not bind CHMP3 and CHMP6 (*27*, *28*). Although little is known about structural properties of MIT domains of calpain-7, differences in binding specificities to ESCRT-III- and ESCRT-III-related proteins are found in comparison with lower eukaryotic calpain-7 orthologues. PalB has a single MIT domain and binds Vps24 (orthologue of CHMP3) (*36*). Although yeast Rim13p has been shown to interact with Vps32p (also named Snf7p, orthologue of CHMP4) by the yeast two-hybrid assays (*37*), it lacks an apparent MIT domain.

MIT domains are found in several cytoplasmic proteins involved in the endosomal sorting system, retrovirus budding, cytokinesis and membrane trafficking and interact with ESCRT-III- and ESCRT-III-related proteins by recognizing short sequences called MIT-interacting motifs (MIMs) located in their C-terminal regions. MIT domains are composed of three helices in a bundle (Helices 1, 2 and 3). Elucidation of 3D structures of MIT–MIM complexes has revealed diversity in MIT–MIM interactions. MIM1 (amphipathic helix) of CHMP1B and MIM2 (Pro-rich strand) of CHMP6 bind to a different groove formed by two helices of VPS4A MIT: MIM1, Helices 2 and 3; MIM2, Helices 1 and 3 (*7–9*, *33*). On the other hand, spastin MIT binds to α6 of CHMP1B with a mode different from binding of VPS4 MIT to MIM1: α6 bound between Helices 1 and 2 (*32*). Although CHMP5 lacks a discernible MIM in its C-terminal region and does not interact with the MIT domain of VPS4, it binds to LIP5MIT via its fifth α-helix (*38*). We found that CL7MIT does not recognize the conventional MIMs in the sixth α-helix (α6) of CHMP1B but binds to α2 in *in vitro* binding experiments using cell lysates (Fig. 4). Although the detected signal was much weaker than the full-length CHMP1B, this is the first evidence that CL7MIT is unique among MIT domains in binding to an N-terminal α-helical region of CHMP1B.

The interaction of GST-CL7MIT with FLAG-CHMP1BΔMIM or FLAG-CHMP1BΔα6 was stronger than that of wild-type FLAG-CHMP1B (Fig. 3, Supplementary Fig. 1). Deletion of the C-terminal region from CHMP1B, mimicking the effect of binding of MIT domains to MIMs, may transform its structure into open conformation (*7*, *32–35*). However, using recombinant proteins of both GST-CHMP1BΔMIM and CL7MIT, no interaction was observed between CHMP1BΔMIM and CL7MIT (Fig. 5). Discrepancy between the results of GST pull-down experiments using cell lysates (enhancing effect by deletion of MIM, Fig. 3) and recombinant proteins (no effect by deletion of MIM, Fig. 5) may be due to the presence of cellular factor(s). Co-immunoprecipitation assays demonstrated that the interaction of CL7MIT with CHMP1B became stronger when IST1 was also coexpressed, suggesting IST1 is such a cellular factor involved in CL7MIT–CHMP1B interaction (Fig. 6).

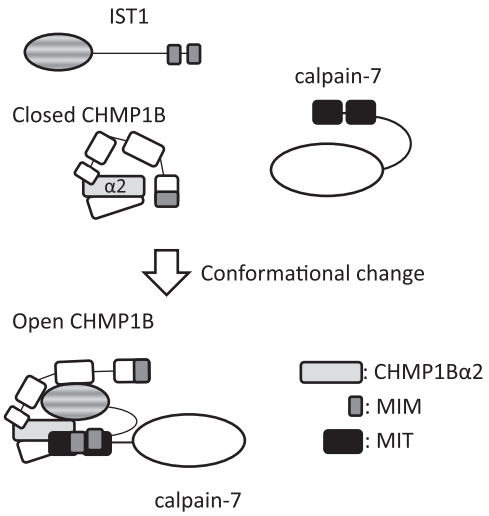

Fig. 8 Binding model for ternary complex of calpain-7, CHMP1B and IST1. Calpain-7-binding site in the second α-helical region in CHMP1B is sequestered in the closed form of CHMP1B. When IST1 binds to CHMP1B, conformational change occurs in CHMP1B, and the second α-helical region (α2) starts to interact with CL7MIT. CL7MIT interacts with both CHMP1Bα2 and IST1MIM. At least those three binding surfaces may contribute to stabilization of the ternary complex.

Based on results of mutational and structural analyses of CHMP3, α5 and the N-terminal side of α2 were reported to be involved in auto-inhibition (*35*). Results of the pull-down assays of CL7MIT with GST-CHMP1BΔNt and GST-CHMP1Bα1-4 lacking putative important amino acids for auto-inhibition agreed with the proposed auto-inhibition model of CHMP proteins. To summarize the results of the present study, we depict a model as shown in Fig. 8. In this model, a calpain-7-binding site in the second α-helical region in CHMP1B (α2) may be sequestered in the closed form of CHMP1B. Binding of IST1 to CHMP1B opens the binding site to be accessible to CL7MIT. Since IST1 also binds CL7MIT, IST1 may function as an adaptor that bridges CHMP1B and calpain-7. In our previous studies, we detected direct interaction between IST1MIM1, 2 and CL7MIT by *in vitro* binding assays (*27*). Regardless of deletion or mutation of MIM1 and MIM2 in IST1, interaction between IST1ΔMIM1, 2 and CL7MIT was not completely abolished, with faint signals for interaction still being observed in co-immunoprecipitation assays using cells expressing FLAG-IST1 mutants and CL7MIT fused with mGFP (*27*). According to our model, endogenous CHMP1B is involved in this interaction. These mutual interactions proposed in this model may stabilize this ternary complex and influence conformation and activities of calpain-7. Indeed, coexpression of CHMP1B and IST1 enhanced autolysis

and increased interaction of calpain-7 synergistically (Figs 2 and 6). Almost the same stoichiometric intensity of immunoreactive signals of bands for FLAG-IST1 and FLAG-CHMP1B in Fig. 6 indicate that CHMP1B/IST1 complex may contribute to ternary complex formation. Mutational analyses based on 3D structures of CHMP3 show that amino acids in α2 near the α1–α2 hairpin and those in α5 are involved in the conformational change of CHMP3 (*6*). This is partly consistent with the results of our *in vitro* interaction analyses showing that the interactions of α2- and α5-containing constructs (full-length and ΔMIM) of CHMP1B with CL7MIT were inhibited but that the interactions of those constructs lacking either α1–α2 hairpin (ΔNt) or α5 (α1–4, α1–3 and α1–2) with CL7MIT were activated (Fig. 5). However, in the pull-down assays using cell lysates, deletion of MIM was sufficient to activate the binding (Fig. 3). To investigate the role of α5 in CL7MIT binding, we expressed mGFP-CHMP1Bα1-4 in cells. However, the expressed protein was recovered in the detergent-insoluble pellet fraction (data not shown). These results suggested that α5 and α6 contribute to a stepwise conformational change of CHMP1B.

Although yeast Ist1p bound to MIM of Did2p (yeast homologue of CHMP1B) (*30*), FLAG-CHMP1BΔα6 interacted with mGFP-IST1 more efficiently than did full-length CHMP1B in our co-immunoprecipitation assay (Supplementary Fig. 3). This result indicated that MIM1 in CHMP1B was dispensable for CHMP1B to interact with IST1 and suggested that the deletion of α6 affected the conformation of CHMP1B. Although the binding site in CHMP1B for IST1 interaction was reported to be located between 61 and 156 amino acids, a more precise binding site was not determined (*11*). We used our single α-helix mutants of CHMP1B for a co-immunoprecipitation assay with IST1, but no α-helix showed interaction with IST1 in our experimental conditions (Supplementary Fig. 4). A larger structural surface of CHMP1B may be necessary for IST1 interaction (*5*). On the other hand, a short amino acid sequence in α2 in CHMP1B may be sufficient for CL7MIT interaction with CHMP1B (Fig. 4).

Our ternary complex model explains how CHMP1B interacts with MIT domains of calpain-7 by the presence of IST1. In parallel, calpain-7 may be catalytically activated in this ternary complex. A pattern of autolytic fragments was changed by coexpression of FLAG-IST1 (Fig. 2). Although the exact cleavage sites have not been determined yet, 30- and 45-kDa fragments (designated 30K and 45K, respectively) were estimated to be generated by cleavage near the C-terminal ends of mGFP and the MIT domains, respectively, in our previous study (*27*), whereas cleavage at somewhere in the protease domain may generate 60K based on apparent molecular weight estimated by SDS–PAGE. Thus, cleavages for 30K and 45K may occur by inter- and/or intra-molecular events, but 60K should be exclusively generated by intermolecular proteolysis. This interpretation is partly supported by the results of exogenous coexpression of both mGFP-fused and Strep-tagged wild-type and catalytically inactive mutants of calpain-7 (substitution of active-site cysteine with serine, C290S) (Supplementary Fig. 5). Fragments (60K and 30K) detected by WB using anti-GFP antibody were generated under coexpression of cofactors (FLAG-IST1 and FLAG-CHMP1B or FLAG-CHMP1BΔα6) by limited proteolysis of mGFP-calpain-7^{C290S} (substrate) with Strep-tagged calpain-7 (enzyme) but not with Strep-calpain-7^{C290S}. The relative amounts of 60K–30K generated by Strep-calpain-7 (enzyme) were greater than those by mGFP-calpain-7 (enzyme and substrate) when FLAG-IST1 was co-overexpressed with FLAG-CHMP1B or FLAG-CHMP1BΔα6. Intermolecular cleavage of mGFP-calpain-7^{C290S} by Strep-calpain-7 was also observed for generation of 45K by overexpressing FLAG-CHMP1BΔα6 in the absence of FLAG-IST1 (data not shown). Recombinant IST1 protein is reported to exist in monomer but also form dimer and oligomer depending on ionic concentrations (*6*), Since IST1 alone can bind CL7MIT (Fig. 5), activated calpain-7 as 'enzyme' and inter-molecularly cleavable calpain-7 as 'substrate' may have different conformations due to differences in binding proteins (IST1/CHMP1B dimer, IST1 of either monomer or dimer/oligomer). Indeed, FLAG-ISTI was estimated to be expressed in 2–3 fold molar excess over coexpressed FLAG-CHMP1B or FLAG-CHMP1BΔα6 in the transfected cells as shown by WB using anti-FLAG antibody (Fig. 2, lower panels). The 45K-cleavage site in mGFP-calpain-7 might be blocked by IST1 dimer/oligomer. Alternatively, 45K becomes highly sensitive to further cleavage at the 30K-cleavage site and rapidly disappears.

Since the ternary complex of mGFP-calpain-7/FLAG-IST1/FLAG-CHMP1B is much more stable than the binary complexes of mGFP-calpain-7/IST1 and mGFP-calpain-7/CHMP1B (Fig. 6), autolytic activity of mGFP-calpain-7 may be enhanced most effectively by interaction with both IST1 and CHMP1B, and the degree of enhancement may be influenced by the relative amounts of these three proteins. We presume that amount of endogenous IST1 is in far excess of CHMP1B based on failure in detection of CHMP1B by WB using specific antibodies (Fig. 7 and Supplementary Fig. 6). In comparison with the amounts of FLAG-tagged proteins, the amount of endogenous calpain-7 seems equal to or slightly less than that of IST1. Overexpression of FLAG-CHMP1BΔα6 alone, however, significantly enhanced the autolysis regardless of plausible shortage of IST1 (Fig. 2B). This fact apparently disagrees with the proposed ternary complex model. Although CHMP1B is the scarce cellular factor, CHMP1A, the closest paralogue of CHMP1B, may substitute for ternary complex formation to some extent. The IST1/CHMP1B binary complex may dissociate from the ternary complex, rebind to free calpain-7 and enhance autolysis either inter-molecularly or intra-molecularly. The IST1/CHMP1BΔα6 complex seems more stable than IST1/CHMP1B complex (Supplementary Fig. 3) and might have a greater turnover rate of dissociation from the processed calpain-7 and re-association with the unprocessed enzyme for autolysis in the cells, where other

unknown cellular factors might be also involved. Overexpression of FLAG-IST1 and FLAG-CHMP1B did not cause apparent autolysis of endogenous calpain-7 but induced translocation of calpain-7 to membrane/organelle fractions (Fig. 7). This translocation of enzyme may increase chances to proteolyse potential substrates that are also recruited to the membrane by binding to scaffold formed by ESCRT and its associating proteins. However, activation of calpain-7 itself for intra-molecular autolysis may not need such membrane translocations. Binding of these ESCRT-III family member proteins to both enzyme and substrates hampers analyses of proteolytic activation. The finding of CHMP1B as a novel co-factor synergistically enhancing calpain-7 autolysis may contribute to the search for calpain-7 substrates in the future. Identification of endogenous substrates would clarify the effects of overexpression of IST1, CHMP1B and their mutants on activation of calpian-7 by clearly distinguishing enzyme and substrates.

Supplementary Data

Supplementary data are available at *JB* online.

Funding
Grant-in-Aid for Scientific Research on Priority Areas (to M.M.; 21025014); Grant-in-Aid for JSPS Fellows (to Y.O., 21-6274).

Conflict of interest
None declared.

Acknowledgements

We thank R. Tanaka for preparation of anti-CHMP1B antibody. We also thank Dr. K. Hitomi and all members of the Laboratory of Molecular and Cellular Regulation for valuable suggestions and discussion.

References

1. Saksena, S., Sun, J., Chu, T., and Emr, S.D. (2007) ESCRTing proteins in the endocytic pathway. *Trends. Biochem. Sci.* **32**, 561–573
2. Williams, R.L. and Urbé, S. (2007) The emerging shape of the ESCRT machinery. *Nat. Rev. Mol. Cell. Biol.* **8**, 355–368
3. McDonald, B. and Martin-Serrano, J. (2009) No strings attached: the ESCRT machinery in viral budding and cytokinesis. *J. Cell. Sci.* **122**, 2167–2177
4. Scott, A., Chung, H.Y., Gonciarz-Swiatek, M., Hill, G.C., Whitby, F.G., Gaspar, J., Holton, J.M., Viswanathan, R., Ghaffarian, S., Hill, C.P., and Sundquist, W.I. (2005) Structural and mechanistic studies of VPS4 proteins. *EMBO J.* **24**, 3658–3669
5. Muziol, T., Pineda-Molina, E., Ravelli, R.B., Zamborlini, A., Usami, Y., Göttlinger, H., and Weissenhorn, W. (2006) Structural basis for budding by the ESCRT-III factor CHMP3. *Dev. Cell.* **10**, 821–830
6. Bajorek, M., Schubert, H.L., McCullough, J., Langelier, C., Eckert, D.M., Stubblefield, W.M., Uter, N.T., Myszka, D.G., Hill, C.P., and Sundquist, W.I. (2009) Structural basis for ESCRT-III protein autoinhibition. *Nat. Struct. Mol. Biol.* **16**, 754–762
7. Obita, T., Saksena, S., Ghazi-Tabatabai, S., Gill, D.J., Perisic, O., Emr, S.D., and Williams, R.L. (2007) Structural basis for selective recognition of ESCRT-III by the AAA ATPase Vps4. *Nature* **449**, 735–739
8. Stuchell-Brereton, M.D., Skalicky, J.J., Kieffer, C., Karren, M.A., Ghaffarian, S., and Sundquist, W.I. (2007) ESCRT-III recognition by VPS4 ATPases. *Nature* **449**, 740–744
9. Kieffer, C., Skalicky, J.J., Morita, E., De Domenico, I., Ward, D.M., Kaplan, J., and Sundquist, W.I. (2008) Two distinct modes of ESCRT-III recognition are required for VPS4 functions in lysosomal protein targeting and HIV-1 budding. *Dev. Cell* **15**, 62–73
10. Bajorek, M., Morita, E., Skalicky, J.J., Morham, S.G., Babst, M., and Sundquist, W.I. (2009) Biochemical analyses of human IST1 and its function in cytokinesis. *Mol. Biol. Cell* **20**, 1360–1373
11. Agromayor, M., Carlton, J.G., Phelan, J.P., Matthews, D.R., Carlin, L.M., Ameer-Beg, S., Bowers, K., and Martin-Serrano, J. (2009) Essential role of hIST1 in cytokinesis. *Mol. Biol.Cell* **20**, 1374–1387
12. Goll, D.E., Thompson, V.F., Li, H., Wei, W., and Cong, J. (2003) The calpain system. *Physiol. Rev.* **83**, 731–801
13. Sorimachi, H. and Suzuki, K. (2001) The structure of calpain. *J. Biochem.* **129**, 653–664
14. Sorimachi, H., Hata, S., and Ono, Y. (2011) Impact of genetic insights into calpain biology. *J. Biochem.* (in press)
15. Hosfield, C.M., Elce, J.S., Davies, P.L., and Jia, Z. (1999) Crystal structure of calpain reveals the structural basis for Ca^{2+}-dependent protease activity and a novel mode of enzyme activation. *EMBO J.* **18**, 6880–6889
16. Strobl, S., Fernandez-Catalan, C., Braun, M., Huber, R., Masumoto, H., Nakagawa, K., Irie, A., Sorimachi, H., Bourenkow, G., Bartunik, H., Suzuki, K., and Bode, W. (2000) The crystal structure of calcium-free human m-calpain suggests an electrostatic switch mechanism for activation by calcium. *Proc. Natl. Acad. Sci. USA.* **97**, 588–592
17. Moldoveanu, T., Hosfield, C.M., Lim, D., Jia, Z., and Davies, P.L. (2003) Calpain silencing by a reversible intrinsic mechanism. *Nat. Struct. Biol.* **10**, 371–378
18. Arthur, J.S., Elce, J.S., Hegadorn, C., Williams, K., and Greer, P.A. (2000) Disruption of the murine calpain small subunit gene, Capn4: calpain is essential for embryonic development but not for cell growth and division. *Mol.Cell. Biol.* **20**, 4474–4481
19. Huang, Y. and Wang, K.K.W. (2001) The calpain family and human disease. *Trend. Mol. Med.* **7**, 355–362
20. Dutt, P., Croall, D.E., Arthur, J.S., Veyra, T.D., Williams, K., Elce, J.S., and Greer, P.A. (2006) m-Calpain is required for preimplantation embryonic development in mice. *BMC Dev. Biol.* **6**, doi:10.1186/1471-213X-6-3
21. Futai, E., Kubo, T., Sorimachi, H., Suzuki, K., and Maeda, T. (2001) Molecular cloning of PalBH, a mammalian homologue of the Aspergillus atypical calpain PalB. *Biochim. Biophys. Acta* **1517**, 316–319
22. Denison, S.H., Orejas, M., and Arst, H.N. Jr. (1995) Signaling of ambient pH in Aspergillus involves a cysteine protease. *J. Biol. Chem.* **270**, 28519–28522
23. Peñalva, M.A. and Arst, H.N. Jr (2002) Regulation of gene expression by ambient pH in filamentous fungi and yeasts. *Microbiol. Mol. Biol. Rev.* **66**, 426–446
24. Peñalva, M.A. and Arst, H.N. Jr (2004) Recent advances in the characterization of ambient pH regulation of gene expression in filamentous fungi and yeasts. *Annu. Rev. Microbiol.* **58**, 425–451

25. Futai, E., Maeda, T., Sorimachi, H., Kitamoto, K., Ishiura, S., and Suzuki, K. (1999) The protease activity of a calpain-like cysteine protease in Saccharomyces cerevisiae is required for alkaline adaptation and sporulation. *Mol. Gen. Genet*. **260**, 559–568
26. Hayashi, M., Fukuzawa, T., Sorimachi, H., and Maeda, T. (2005) Constitutive activation of the pH-responsive Rim101 pathway in yeast mutants defective in late steps of the MVB/ESCRT pathway. *Mol. Cell. Biol.* **25**, 9478–9490
27. Osako, Y., Maemoto, Y., Tanaka, R., Suzuki, H., Shibata, H., and Maki, M. (2010) Autolytic activity of human calpain 7 is enhanced by ESCRT-III-related protein IST1 through MIT-MIM interaction. *FEBS J*. **277**, 4412–4426
28. Yorikawa, C., Takaya, E., Osako, Y., Tanaka, R., Terasawa, Y., Hamakubo, T., Mochizuki, Y., Iwanari, H., Kodama, T., Maeda, T., Hitomi, K., Shibata, H., and Maki, M. (2008) Human calpain 7/PalBH associates with a subset of ESCRT-III-related proteins in its N-terminal region and partly localizes to endocytic membrane compartments. *J. Biochem* **143**, 731–745
29. Rue, S.M., Mattei, S., Saksena, S., and Emr, S.D. (2008) Novel Ist1-Did2 complex functions at a late step in multivesicular body sorting. *Mol. Biol. Cell* **19**, 475–484
30. Xiao, J., Chen, X.W., Davies, B.A., Saltiel, A.R., Katzmann, D.J., and Xu, Z. (2009) Structural basis of Ist1 function and Ist1-Did2 interaction in the multivesicular body pathway and cytokinesis. *Mol. Biol. Cell* **20**, 3514–3524
31. Katoh, K., Shibata, H., Suzuki, H., Nara, A., Ishidoh, K., Kominami, E., Yoshimori, T., and Maki, M. (2003) The ALG-2-interacting protein Alix associates with CHMP4b, a human homologue of yeast Snf7 that is involved in multivesicular body sorting. *J. Biol. Chem.* **278**, 39104–39113
32. Yang, D., Rismanchi, N., Renvoisé, B., Lippincott-Schwartz, J., Blackstone, C., and Hurley, JH. (2008) Structural basis for midbody targeting of spastin by the ESCRT-III protein CHMP1B. *Nat. Struct. Mol. Biol.* **15**, 1278–1286
33. Scott, A., Gaspar, J., Stuchell-Brereton, M.D., Alam, S.L., Skalicky, J.J., and Sundquist, W.I. (2005) Structure and ESCRT-III protein interactions of the MIT domain of human VPS4A. *Proc. Natl. Acad. Sci. USA* **102**, 13813–13818
34. Shim, S., Kimpler, L.A., and Hanson, P.I. (2007) Structure/function analysis of four core ESCRT-III proteins reveals common regulatory role for extreme C-terminal domain. *Traffic* **8**, 1068–1079
35. Lata, S., Roessle, M., Solomons, J., Jamin, M., Gottlinger, H.G., Svergun, D.I., and Weissenhorn, W. (2008) Structural basis for autoinhibition of ESCRT-III CHMP3. *J. Mol. Biol.* **9**, 818–827
36. Rodríguez-Galán, O., Galindo, A., Hervás-Aguilar, A., Arst, H.N. Jr, and Peñalva, M.A. (2009) Physiological involvement in pH signaling of Vps24-mediated recruitment of Aspergillus PalB cysteine protease to ESCRT-III. *J. Biol. Chem.* **284**, 4404–4412
37. Ito, T., Chiba, T., Ozawa, R., Yoshida, M., Hattori, M., and Sakaki, Y. (2001) A comprehensive two-hybrid analysis to explore the yeast protein interactome. *Proc. Natl. Acad. Sci. USA* **98**, 4569–4574
38. Shim, S., Merrill, S.A., and Hanson, P.I. (2008) Novel interactions of ESCRT-III with LIP5 and VPS4 and their implications for ESCRT-III disassembly. *Mol. Biol. Cell* **19**, 2661–2672